HOST ROCKS, HYDROTHERMAL ALTERATION PATTERNS, AND MINERALIZATION STYLES OF THE JAGUAR NORTE DEPOSIT IN THE SOUTHERN COPPER BELT, CARAJÁS PROVINCE

Laryssa de Sousa Carneiro[1]; Carolina P. N. Moreto[1]; Lena V. S. Monteiro[2]; Marco A. Delinardo da Silva[3]; Ezequiel Pozocco[4]; Juliana Araujo[4]; Ivandro Schoenherr[4]; Gustavo Diniz Oliveira[4]; Fernando M. V. Matos[5]

[1]University of Campinas - UNICAMP; [2] University of São Paulo - USP; [3]Federal University of Uberlândia - UFU; [4]VALE S.A.; [5]SERVIGEO Geologia e Geofísica LTDA

laryssa.s.carneiro@gmail.com; cmoreto@unicamp.br; lena.monteiro@usp.br; marco.delinardo@ufu.br; ezequiel.pozocco@vale.com; juliana.araujo@vale.com; ivandro.prado@vale.com; gustavo.diniz.oliveira@vale.com; fmartins5@hotmail.com

ABSTRACT

The Jaguar Norte Cu-Ni deposit is situated along the intersection between the Canaã shear system and the NE-SW McCandless fault in the southwestern sector of the Carajás Domain, Pará. The deposit is hosted by foliated metatonalite-granodiorite, metamafic-ultramafic, and subvolcanic rocks crosscut by porphyritic granite and pegmatite intrusions. The hydrothermal alteration stages include sodic, sodic-calcic, potassic, calcic-iron, and potassic-iron or biotite-chlorite-magnetite alteration. In mafic-ultramafic rocks, veins with talc-serpentine-magnetite±actinolite-apatite form a mesh or bastite texture. The copper-nickel ore in both foliated granitoid (chalcopyrite-pyrite-pentlandite-molybdenite-pyrrhotite) and mafic-ultramafic rocks (pyrrhotite-chalcopyrite-pyrite-pentlandite-sphalerite) is controlled by ductile fabrics. Veins and veinlets with epidote-carbonate-hematite and potassic-iron alteration with chalcopyrite represent an overprinting episode of mineralization. The geological setting and hydrothermal alteration patterns of the Jaguar Norte deposits are similar to the Carajás Province IOCG deposits. It may represent a Ni-rich member within the IOCG system.

PALAVRAS-CHAVE: Ni-rich IOCG deposits; Hydrothermal alteration; Carajás Province.

INTRODUCTION

The Carajás Province is worldwide recognized for hosting numerous copper deposits, including world-class iron oxide-copper-gold (IOCG). The mineralization and hydrothermal alteration patterns of these deposits are structurally controlled by E-W and WNW-ESE trending shear zones, defining the Northern Copper Belt (Cinzento Shear Zone) and the Southern Copper Belt (Canaã Shear Zone) (Xavier et al. 2012). The genesis of these deposits has been attributed to multiple hydrothermal events during the Neoarchean (ca. 2.70 to 2.68 Ga; ca. 2.5 Ga) and Paleoproterozoic (ca. 2.05 Ga; ca. 1.88 Ga) (Moreto et al. 2015a, 2015b).

The Jaguar Norte Cu-Ni deposit belongs to Vale S.A. company, and is located in the southwestern sector of the Carajás Domain, along the intersection between the Canaã shear system and the NE-SW McCandless fault. This deposit occurs near the Serra do Puma and Onça

mafic-ultramafic complexes (Macambira and Ferreira Filho 2002; Ferreira Filho *et al*. 2007) to the north of Jaguar hydrothermal Ni deposit (Ferreira Filho *et al.* 2021).

In this contribution, we present new geological data based on regional geology, detailed drill core and petrographic description in order to constrain the host rocks, hydrotermal alteration system, and ore assemblages and styles of the Jaguar Norte deposit deposit. We show that it shares several similarities with the Carajás IOCG deposits, including structural control by regional discontinuities, and intense Fe and alkali hydrothermal alteration.

MATERIAL AND METHODS

The geological characterization of the Jaguar Norte deposit was based on drill core logging, geological mapping, and petrographic studies. Detailed macroscopic and petrographic descriptions of two drill cores (PKS JAGN DH00005 and PKS JAGN DH00019) and of samples collected on a regional geological survey allowed defining the nature of the host and regional rocks, identifying the styles and distribution of hydrothermal alteration zones and mode of occurrence of the Cu-Ni mineralization. Representative samples (n = 29) were chosen for optical microscopic analysis, performed at the Institute of Geosciences, University of Campinas (UNICAMP).

RESULTS

The Jaguar Norte Cu-Ni deposit is located approximately 6 km north of the Serra Arqueada iron deposit, 4 km NW of the Serra do Puma Complex, 10 km NE of the Serra da Onça Complex, and approximately 2 km north of the Jaguar deposit. The Jaguar Norte mineralization and associated hydrothermal alteration are structurally controlled by two important regional discontinuity systems, the E-W Canaã fault system and the NE-SW McCandless fault, occurring along the intersection of these structures.

Geological units mapped in the area include Mesoarchean rocks of the Xingu Complex, banded iron formation of the Serra Arqueada, metavolcanosedimentary sequences, granite intrusions and mafic-ultramafic complexes. The Xingu Complex is represented by banded felsic gneisses and migmatites with stromatic to vein and schlieren structure. Meta-banded iron formation exhibits slight folding and commonly amphibole and garnet-rich hydrothermal alteration zones. The subvolcanic rocks of the Itacaiúnas Supergroup are felsic to intermediate, with equigranular to porphyritic texture. The granite rocks in the area are medium-grained isotropic to weakly foliated granodiorite, likely related to the Neoarchean Plaquê Suite. Mafic and ultramafic intrusions include the Serra do Puma and Serra da Onça Complexes (Macambira and Ferreira Filho, 2002; Ferreira Filho *et al.,* 2007), which host the world-class Puma-Onça lateritic nickel deposit.

The Jaguar Norte deposit is hosted by foliated meta-tonalite to meta-granodiorite (Fig. 1A-B), meta-mafic-ultramafic rocks (Fig 1C-D), porphyritic intermediate to felsic subvolcanic rocks (Fig. 1E-F), and inequigranular to porphyritic granite (Fig. 1G) and pegmatite (Fig.1H) intrusions.

The host meta-tonalite and biotite-granodiorite are light to dark gray, medium-grained (500 µm to 3 mm), isotropic to foliated rocks composed of plagioclase (48-60%), quartz (20%), and minor orthoclase (up to 10%), with accessory biotite (15-18%), magnetite and hydrothermal albite (I), K-feldspar (I), biotite (I), and chlorite (I) (Fig. 1A-B). These rocks have equigranular, interlobate to hypidiomorphic texture with evidence of dynamic recrystallization of quartz and feldspar. Anastomosed, incipient and spaced foliation (S_n) is defined by the preferential orientation of biotite. Non-foliate domains are marked by polygonal to ameboid quartz that exhibits patchy and undulose extinction and lamellae deformation. Plagioclase crystals show tapering and bent twinning planes, core-and-mantle structure and microfractures associated with plastic-mismatches. Shearing zones are associated with a mylonite foliation (S_{n+1}) defined by parallel biotite-K-feldspar-muscovite-rich zones together with quartz comminution and stretching.

Meta-ultramafic rocks are reddish, dark green or black (Fig. 1C). They may exhibit preserved cumulative texture, with olivine and pyroxene pseudomorphs. These rocks are partly to completely serpentinized and show pseudomorphic mesh and bastite textures developed by chlorite-serpentine-magnetite veinlets. Locally, there are mylonitized sectors (Fig. 1D) with talc-tremolite-actinolite zones in well-developed foliation.

The host felsic to intermediate subvolcanic rocks are massive, light brownish gray to dark gray, isotropic to foliated, and porphyritic rocks (Fig.1E-F). The fine-grained matrix (~100µm) is composed of quartz, alkali feldspar, plagioclase, and subordinate biotite and amphibole. Euhedral to subhedral phenocrysts of plagioclase and alkali feldspar are millimeter-scale (1 to 2 mm). In intensely deformed rocks, high content of hydrothermal biotite and titanite is observed, defining the mylonitic foliation (S_{n+1}) and is accompanied by crystal stretching and comminution. These subvolcanic rocks are crosscut by light gray granitic and pegmatitic apophyses with graphic texture associated with sodic (albite) alteration, actinolite and biotite-titanite fronts.

Inequigranular to porphyritic granodiorites to monzogranites are light pinkish gray, isotropic, composed of plagioclase (40-45%), quartz (20%), alkali feldspar (up to 15%), and minor biotite (up to 10 %), chlorite (2%), magnetite (1%), and sericite alteration (Fig. 1G) Pegmatite intrusions are white, light pink, coarse-grained rocks with plagioclase (30%), recrystallized quartz (30%), microcline or orthoclase (20%), and accessory biotite (10%), chlorite (5%), and amphibole (5%) (Fig.1H). Both granite and pegmatite intrusions crosscut the foliated granodiorite and mafic-ultramafic rocks. These rocks are commonly associated with late albite and potassic-iron (K-feldspar, biotite, hematite) alterations, carbonate-epidote-hematite veins and chalcopyrite veinlets (Fig. 1G).

Hydrothermal alteration is developed especially on granitic rocks and occurs on S_n and S_{n+1} foliation planes, mainly in fronts of selective and pervasive alteration that increase in intensity towards shear zones, often accompanied by crystal stretching, folding and deformation. The hydrothermal system is characterized by an early sodic alteration (albite I) (Fig. 1A), followed by sodic-calcic (albite-actinolite-apatite), potassic (biotite I-K-feldspar I) (Fig. 1K-L), calcic-iron (actinolite-magnetite-apatite), and potassic-iron (biotite II-magnetite) (Fig. 1M-N) or biotite-chlorite-magnetite-apatite (Fig. 1O-P) alteration. In ultramafic and mafic rocks, assemblages rich in talc-serpentine-magnetite±actinolite-apatite in a mesh or bastite fabric (Fig. 1C) obliterate the initial texture and composition of the rocks and are followed by biotite-actinolite-apatite, biotite-chlorite, and actinolite-magnetite-apatite (Ca-Fe) alteration zones.

The copper mineralization is mainly formed by disseminated chalcopyrite crystals, vein, massive, and ore breccias zones (Fig. 1I). Chalcopyrite (I) is associated with magnetite-rich rocks and occurs in strings controlled by the mylonite foliation (Fig. 1I) defined by actinolite, biotite, and chlorite stretching and folding (Fig. 1Q-R). Pyrite, pentlandite, molybdenite, and pyrrhotite are associated with these copper-rich zones. Pyrrhotite is the main sulfide in altered mafic-ultramafic rocks (Fig. 1J), mainly associated with actinolite-magnetite, pyrite, chalcopyrite (I), pentlandite and sphalerite. Chalcopyrite (II) also occurs in late carbonate-epidote-hematite and potassic-iron (K-feldspar-biotite-hematite) veins.

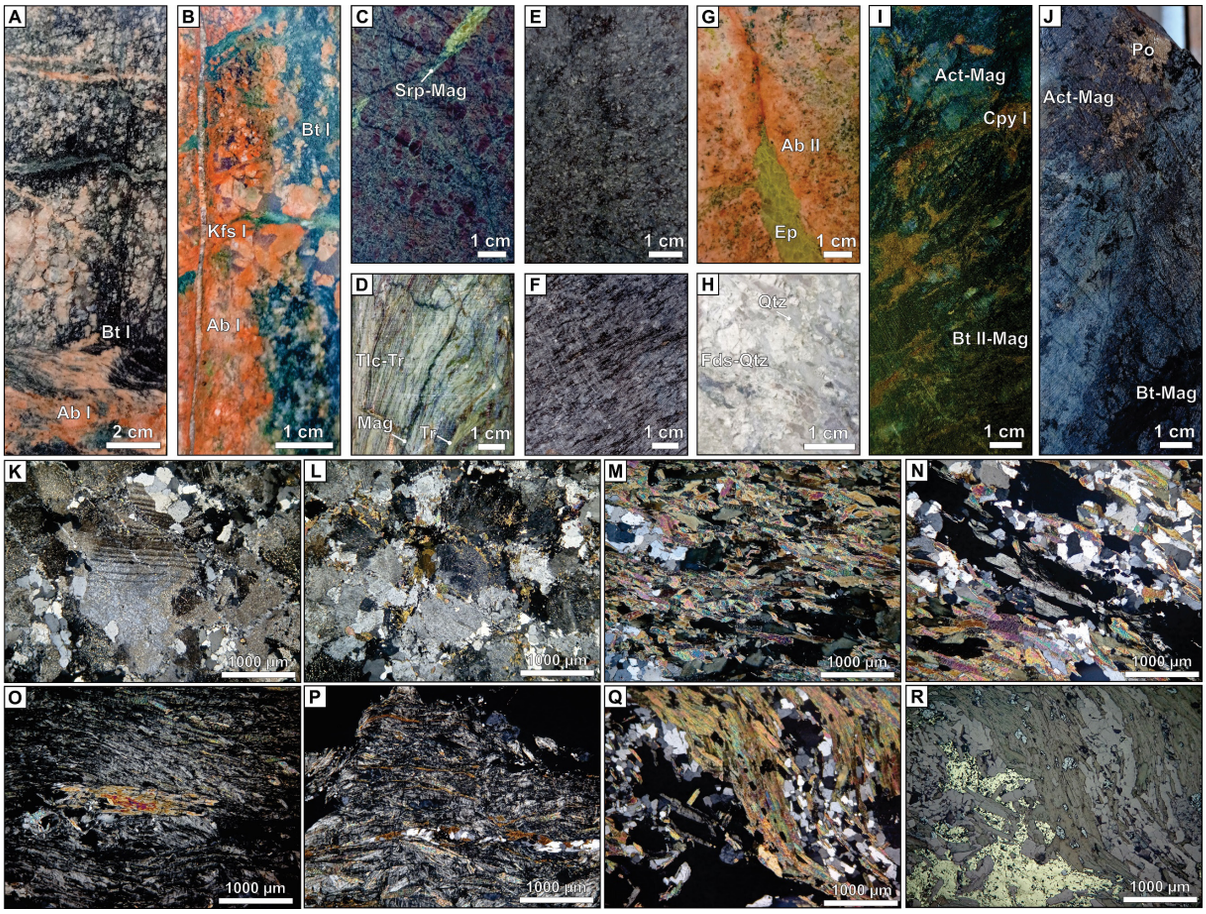

Figure 1. Petrographic features of the main host rocks, hydrothermal alteration and mineralization of the Jaguar Norte deposit. A-B: sodic and potassic alteration in foliated granodiorite. C-D: altered ultramafic rocks. E-F: isotropic to foliated subvolcanic rocks. G-H: inequigranular granite and pegmatite intrusions. I: chalcopyrite (I) along mylonitic foliation. J: pyrrhotite-magnetite in altered ultramafic rock. K-L: potassic alteration (orthoclase-biotite). M-N: iron-potassic alteration. O-P: chlorite-magnetite-apatite alteration. Q-R: chalcopyrite (I) in stretched and folded biotite hinge.

DISCUSSION AND CONCLUSIONS

The host rocks of the Jaguar Norte deposit are altered by sodic, sodic-calcic, potassic, calcic-iron, potassic-iron or biotite-chlorite-magnetite hydrothermal assemblages that occur along foliation (S_n and S_{n+1}), mainly controlled by ductile deformation, and that obliterate the initial texture and composition of the rocks. The ore is essentially composed of chalcopyrite (I) (pyrite-pentlandite-molybdenite-pyrrhotite) and pyrrhotite (pyrite-chalcopyrite-pentlandite-

sphalerite) breccias and veins in mylonite foliation. Late mineralization with chalcopyrite (II) is associated with brittle veins and breccias that crosscut previous alteration stages. The location of ore zones along the intersection between the Canaã shear system and the McCandless fault likely provided extensive fluid percolation during the hydrothermal system development.

Although both tonalite-granite intrusions and subvolcanic rocks have preserved igneous paragenesis and texture, they exhibit weakly to intense spaced foliation (S_n) with evidence of dynamic recrystallization. Pegmatite and inequigranular granite are much less deformed, but can show incipient crystal orientation and recrystallization. Intense deformation is associated with parallel to anastomosed continuous mylonitic foliation (S_{n+1}) with dynamic recrystallization and deformation (e.g., folding, stretching, kinking, twin tapering and bent, crystal comminution). The mylonitic foliation (S_{n+1}) forms a network of heterogeneous ductile shear domains likely associated with the development of the Canaã shear system.

Field relationships and petrographic evidence demonstrate that the Jaguar Norte deposit is marked by a complex hydrothermal and deformation evolution. The association with deep regional fault system, the structural control on hydrothermal alteration and ore zones, the intense Fe and Fe-Mg (chlorite) enrichment and alkali metasomatism are similar features to the Carajás IOCG deposits. Copper-nickel mineralization in the Jaguar Norte deposit is closely associated with magnetite-apatite-rich breccias, suggesting that it may represent a Ni-rich IOCG. This deposit also exhibits hydrothermal and geological features similar to the Jaguar hydrothermal Ni deposit (Ferreira Filho et al. 2021)

Acknowledgements

We are grateful to Vale S.A. mining company for their unceasing support. This research is funded by Vale S.A. due to a collaborative project (ADIMB/Vale S.A/Universities). We also would like to thank CAPES for providing a PhD Scholarship (88887.609887/2021-00) to the first author.

REFERENCES

Ferreira Filho C.F., Cançado F., Correa C., Macambira E.M.B., Junqueira-Brod T.C., Siepierski L. 2007. Mineralizações estratiformes de PGE-Ni associadas a complexos acamadados em Carajás: os exemplos de Luanga e Serra da Onça. *In*: Rosa-Costa L.T., Klein E.L., Viglio E.P. (eds.). *Contribuições à geologia da Amazônia*. SBG-Núcleo Norte, Belém, p. 1-14.

Ferreira Filho, C.F.; Oliveira, M.M.F.; Mansur, E.T.; Rosa, W.D. 2021. The Jaguar hydrothermal nickel sulfide deposit: Evidence for a nickel-rich member of IOCG-type deposits in the Carajás Mineral Province, Brazil. *Journal of South American Earth Sciences*, **111:** 103501.

Macambira, E.M.B.; Ferreira Filho, C.F. 2002. Fracionamento magmático dos corpos máficoultramáficos da Suíte Intrusiva Cateté - sudeste do Pará. *In*: Klein, E.L., Vasquez, M.L., Rosa-Costa, L.T. (eds.). *Contribuições à geologia da Amazônia*. Belém, p. 105-114.

Moreto C.P.N.; Monteiro L.V.S.; Xavier R.P.; Creaser R.A., DuFrane S.A., Tassinari C.C.G.; Sato K.; Kemp A.I.S., Amaral W.S. 2015a. Neoarchean and Paleoproterozoic iron oxide-copper-gold events at the Sossego Deposit, Carajás Province, Brazil: Re-Os and U-Pb geochronological evidence. *Economic Geology*, **110:** 809-835.

Moreto C.P.N.; Monteiro L.V.S.; Xavier R.P.; Creaser R.A.; DuFrane A., Melo G.H.C.; Silva M.A.D.; Tassinari C.C.G.; Sato K. 2015b. Timing of multiple hydrothermal events in the iron oxide-copper-gold deposits of the Southern Copper Belt, Carajás Province, Brazil. *Mineralium Deposita*, **50:** 517-546.

Santos, J.O.S. 2003. Geotectônica dos Escudos da Guiana e Brasil Central. *In*: Bizzi, L.A., Schobbenhaus, C., Vidotti, R.M., Gonçalves, J.H., (eds.), *Geologia, Tectônica e Recursos Minerais do Brasil. Texto, Mapas e SIG*. CPRM-Serviço Geológico do Brasil, 4, p. 169-226.

Xavier, R. P., Monteiro, L. V. S., Moreto, C. P. N., Pestilho, A. L. S., Melo, G. D., Silva, M. D., Silva, F. E. 2012. The iron oxide copper-gold systems of the Carajás mineral province, Brazil. *Society of Economic Geologists*, **16:** 433-453.